CCD Photometry and Roche Modeling of the Eclipsing Overcontact Binary Star System TYC 01963-0488-1

Kevin B. Alton
UnderOak Observatory, 70 Summit Avenue, Cedar Knolls, NJ 07927; kbalton@optonline.net

Received May 17, 2016; revised June 7, 2016; accepted June 8, 2016

Abstract TYC 01963-0488-1 (ASAS J094440+2632.1) is a W UMa binary system (P = 0.427036 d) which has been largely overlooked since first being detected nearly 15 years ago by the ROTSE-I telescope. Other than the monochromatic ROTSE-I survey data, no multi-colored light curves have been published. Photometric data collected in three bandpasses (B, V, and I_c) at UnderOak Observatory produced five new times-of-minimum for TYC 01963-0488-1 which were used to establish a linear ephemeris from the first Min I epoch (HJD_0). No published radial velocity data are available for this system; however, since this W UMa binary undergoes very obvious total eclipses, Roche modeling yielded a well-constrained photometric value for q (~0.25). There is a suggestion from the ROTSE-I data and new results herein that Max II is more variable than Max I. Therefore, Roche model fits for the TYC 01963-0488-1 light curves collected in 2015 were assessed with and without spots.

1. Introduction

The variable behavior of TYC 01963-0488-1 was first observed during the ROTSE-I CCD survey (Gettel *et al.* 2006); the system was later classified by Hoffman *et al.* (2009). Photometric data are accessible on the Northern Sky Variable Survey website (Wozniak *et al.* 2004). Other than the reduced on-line data (Gettel *et al.* 2006) at VizieR and an entry in the International Variable Star Index (VSX; Watson *et al.* 2014), no other reference to this binary system was found in the literature. The paper herein marks the first robust determination of orbital period and Roche model assessment of TYC 01963-0488-1 which has been published.

2. Observations and data reduction

2.1. Photometry

Equipment included a 0.28-m catadioptic telescope with an SBIG ST-8XME CCD camera mounted at primary focus. Automated imaging was performed with SBIG photometric B, V, and I_c filters manufactured to match the Bessell prescription. The computer clock was updated immediately prior to each session and exposure time for all images adjusted to 75 seconds. Image acquisition (lights, darks, and flats) was performed using CCDSOFT v5 (Software Bisque 2011) while calibration and registration were performed with AIP4WIN v2.4.0 (Berry and Burnell 2011). Images of TYC 01963-0488-1 were plate-solved using the standard star fields (MPOSC3) provided in MPO CANOPUS v10.7.1.3 (Minor Planet Observer 2015). MPO CANOPUS also provided the means for further photometric reduction to light curves using a fixed ensemble of five non-varying comparison stars in the same field-of-view (FOV). To minimize error due to differential refraction and color extinction, only data from images taken above 30° altitude (airmass < 2.0) were used. Instrumental readings were reduced to catalog-based magnitudes using the MPOSC3 reference star fields built into MPO CANOPUS. Stars in MPOSC3 with BVI_c magnitudes derived from 2MASS J-K magnitudes have an internal consistency of ±0.05 mag. for V, ±0.08 mag. for B, ±0.03 mag. for I_c, and ±0.05 mag. for B–V (Warner 2007).

2.2. Light curve analyses

Roche type modeling was performed with the assistance of BINARY MAKER 3 (BM3; Bradstreet and Steelman 2004), WDWINT5.6A (Nelson 2009), and PHOEBE 0.31a (Prša and Zwitter 2005), the latter two of which employ the Wilson-Devinney (WD) code (Wilson and Devinney 1971; Wilson 1979). Spatial renderings of TYC 01963-0488-1 were also produced by BM3 once model fits were finalized. Times-of-minimum were calculated using the method of Kwee and van Woerden (1956) as implemented in PERANSO v2.5 (Vannmunster 2006).

3. Results and discussion

3.1. Photometry and ephemerides

Five stars in the same FOV with TYC 01963-0488-1 which were used to derive catalog-based (MPOSC3) magnitudes (Table 1) showed no evidence of inherent variability over the period of image acquisition and stayed within ±0.03 magnitude for V and I_c filters and ±0.05 for B. Photometric values in B (n = 407), V (n = 407), and I_c (n = 410) were processed to generate three LCs that spanned 45 days between March 24 and May 8, 2015 (Figure 1). In total, four new secondary (s) and one primary (p) minima were captured during this investigation; data from all filters were averaged for each session (Table 2) since no color dependency on the timings was noted. A period determination (P = 0.427028 ± 0.000008) from unfiltered data (ROTSE-I) collected in 1999–2000 was made using PERANSO (Vanmunster 2006) by applying periodic orthogonals (Schwarzenberg-Czerny 1996) to fit observations and analysis of variance (ANOVA) to evaluate fit quality. After converting magnitude to flux, ROTSE-I and Underoak Observatory (UO) light curve data (V mag.) were then folded together; the best fit was found where the orbital period was 0.427036 ± 0.000004 day (Figure 2). The Fourier routine (FALC) in MPO CANOPUS provided a similar period solution (0.427036 ± 0.000006) using only the multicolor data from UO. The first epoch (HJD_0) for this eclipsing binary is therefore defined by the following linear ephemeris equation:

$$\text{Min. I hel.} = 2457150.63657\ (3) + 0.427036\ (4)\ E \quad (1)$$

Table 1. Astrometric coordinates (J2000) and MPOSC3 catalog magnitudes (B, V, and I_c) for TYC 01963-0488-1 and five comparison stars used in this photometric study.

Star Identification	*R. A. h m s*	*Dec. ° ′ ″*	*MPOSC3[a] B mag.*	*MPOSC3 V mag.*	*MPOSC3 I_c mag.*	*MPOSC3 (B–V)*
TYC 01963-0488-1	09 44 40.44	26 32 07.2	11.57–12.11[b]	11.17–11.63[b]	10.69–11.15[b]	0.399
TYC 01963-0389-1	09 44 44.82	26 39 33.5	12.574	11.830	11.017	0.744
GSC 01963-00146	09 44 52.06	26 42 27.5	13.288	12.685	12.000	0.603
TYC 01963-0461-1	09 44 07.14	26 36 36.9	12.272	11.418	10.508	0.854
GSC 01963-00102	09 44 46.83	26 33 28.5	14.237	13.722	13.120	0.515
GSC 01963-00586	09 44 44.41	26 34 30.3	14.501	13.971	13.355	0.530

a: MPOSC3 is a hybrid catalog which includes a large subset of the Carlsberg Meridian Catalog (CMC-14) as well as from the Sloan Digital Sky Survey (SDSS).
b: Range of observed magnitudes in UO light curves for TYC 01963-0488-1

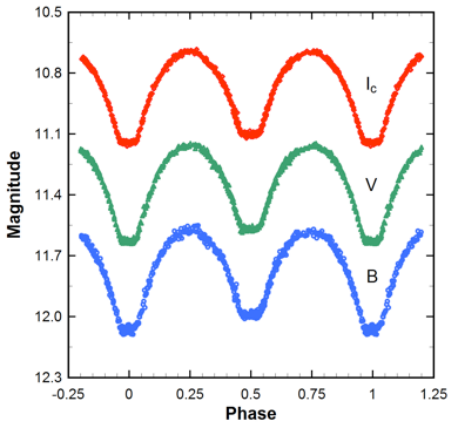

Figure 1. Folded CCD light curves for TYC 01963-0488-1 produced from photometric data obtained between March 24 and May 8, 2015. The top (I_c), middle (V), and bottom curve (B) shown above were reduced to MPOSC3-based catalog magnitudes using MPO CANOPUS.

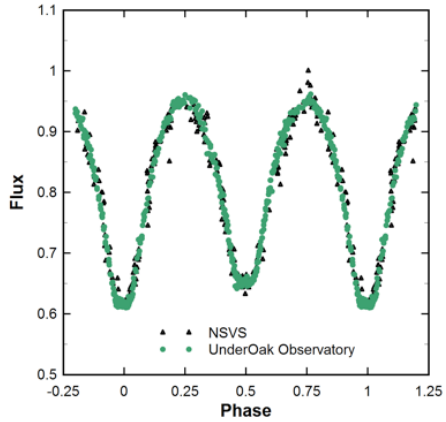

Figure 2. Survey data from the ROTSE-I telescope and photometric results (V mag.) collected at UnderOak Observatory were folded together using period analysis (P = 0.427036 ± 0.000004 d). Greater scatter at Min II (φ = 0.75) suggests the possibility of an active photosphere for TYC 01963-0488-1.

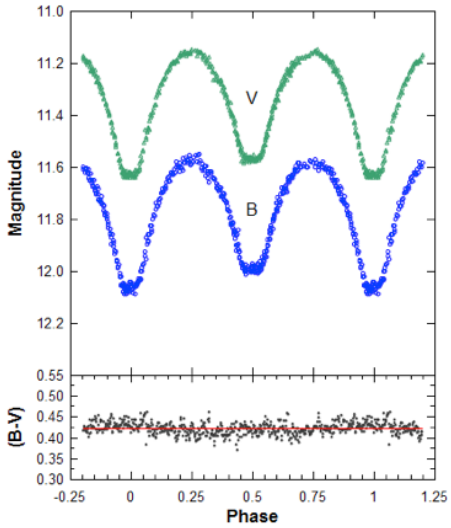

Figure 3. Color change (B–V) of TYC 01963-0488-1 during varying phases of eclipse was evaluated from binned data (φ = 0.002). Relatively minor deviations from the solid-line mean (0.423 ±0.014) suggest that the effective temperatures of both stars are not very different.

Table 2. New times-of-minimum for TYC 01963-0488-1 acquired at UnderOak Observatory.

Mean Observed Time-of-Minimum (HJD–2400000)	*± Error*	*UT Date of Observations*	*Type of Minimum[a]*
57114.5523	0.0002	02Apr2015	s
57117.5433	0.0001	05Apr2015	s
57134.6238	0.0002	22Apr2015	s
57137.6136	0.0001	25Apr2015	s
57150.6366	0.0002	08May2015	p

a: s = secondary; p = primary.

Table 3. Difference in light curve minima and maxima by bandpass.

Band	*Max II – Max I*	*Min I – Min II*	*Min I – Max I*	*Min II – Max II*
B	0.015	0.0739	0.5002	0.4113
V	0.005	0.0581	0.4766	0.4131
I_c	0.004	0.0405	0.4551	0.4110

No attempt was made to determine whether there are secular changes in eclipse timings over time since these data were only collected over 45 days.

3.2. Light curve behavior

As expected from a overcontact binary system, LCs (Figure 1) exhibit minima which are separated by 0.5 phase (φ) and consistent with a synchronous circular orbit. Flattened bottoms at Min I and Min II strongly suggest that this binary system undergoes total eclipses. Data from the ROTSE-I survey tend to exhibit greater variability around Max II compared to Max I (Figure 2). A slightly positive O'Connell effect (Max II fainter than Max I) is observed most notably with the B passband during the 2015 campaign whereas both V and I_c passbands exhibit vanishingly smaller differences (Table 3). In general this effect has been attributed to the presence of cool starspot(s), hot region(s), gas stream impact on either or both of the binary cohorts, and/or other unknown phenomena which produce surface inhomogeneities (Yakut and Eggleton 2005). The net result can be unequal heights during maximum light and is often simulated by the introduction of starspots during Roche-type modeling of the LC data.

3.3. Spectral classification

Data from folded LCs (V- and B-mag) were binned into equal phase intervals (0.002) to produce a difference (B–V) plot (Figure 3). It would appear that changes in color with phase are small (0.423 ± 0.014) suggesting relatively minor differences in effective temperature between stars. Color index (B–V) data from UO and three other surveys (Table 4) were corrected using the reddening value (E(B–V) = 0.0175 ± 0.0005) observed within a 5 arcmin radius of TYC 01963-0488-1 (Schlafly and Finkbeiner 2011; Schlegel *et al.* 1998). The mean result, $(B–V)_0$ = 0.393 ± 0.014, which was adopted for subsequent Roche modeling, indicates that the most luminous star in this system has an effective temperature of 6705 K, and ranges between spectral type F2V and F3V (Pecaut and Mamajek 2013) .

3.4. Roche modeling approach

In the absence of radial velocity (RV) data, it is not possible to unequivocally determine q, the mass ratio (m_2 / m_1), or whether TYC 01963-0488-1 is an A- or W-type overcontact binary system. According to Binnendijk (1970), the deepest minimum (Min I) of an A-type W UMa variable results from the eclipse of the hotter more massive star by the cooler less massive cohort. This is in contrast to W-types where the deepest minimum results from the hotter but less massive star being eclipsed by the more massive but cooler cohort. In general, A-type W UMa variables can be characterized by their total mass ($M_T > 1.8\ M_\odot$), spectral class (A–F), orbital period (P > 0.4 d), extent of thermal contact (*f*), propensity to exhibit a total eclipse due to large size differences, mass ratio (q < 0.3), and the temperature difference (ΔT < 100 K) between the hottest and coolest star (Skelton and Smits 2009). On balance, when all of these factors are considered, TYC 01963 0488-1 would appear to best fit those parameters which define an A-subtype. A reliable photometric value for mass ratio (q_{ph}) can be determined but only for those W UMa systems where a total eclipse is observed from our vantage point (Terrell and Wilson 2005). A recent paper published by Hambálek and Pribulla (2013) offered an approach to estimate mass ratio (q) and the orbital inclination (i) prior to Roche modeling. These investigators employed the code ROCHE (Pribulla 2012) to simulate a total of 11,895 LCs from overcontact binaries as defined by varying values for three parameters (q (0.05–1; Δ = 0.025), fill-out (*f* = 0, 0.25, 0.50, 0.75, 1), and i (30°–90°; Δ=1°)). A LC from an eclipsing binary can be represented by trigonometric polynomials such that the corresponding Fourier coefficients define the "informational contents" of the system. A partial eclipse can be adequately represented by a 10th order trigonometric polynomial, whereas a total eclipse is more difficult to model. In this case only the first 11 Fourier coefficients (a_0–a_{10}) were used to investigate the uniqueness of each solution (Table 5). The amplitude of the LC and the minima width are respectively constrained by the values for a_2 and a_4. The uniqueness (δq) for a photometric mass ratio (q_{ph}) solution is defined by the a_2–a_4 plane (Hambálek and Pribulla 2013) and varies according to the number and precision of the LC data points. The authors have conveniently provided an on-line link to UNIQUE (http://www.ta3.sk/~lhambalek/download/unique.zip), which can be used to calculate the geometric elements [q, *f*, and i] along with the corresponding Fourier coefficients.

In preparation for analysis by UNIQUE, monochromatic LC data (n = 407; V mag.) collected at UO were converted to normalized flux and then binned into constant phase intervals (0.002) to satisfy a requirement of the program. When third light (l_3) was assumed to be zero, the best match from the LC data library (coef.dat) used by UNIQUE corresponded to q = 0.225, *f* = 0.5, and i = 79°. Roche modeling of LC data

Table 4. Spectral classification of TYC 01963-0488-1 based upon dereddened[a] (B–V) data from various surveys and the present study.

Stellar Attribute	*MPOSC3*	*2MASS*	*SDSS-DR8*	*Present Study*
$(B-V)_0$	0.382 ±0.094	0.381 ±0.050	0.407 ±0.04	0.404 ±0.014
T_{eff1}[b] (K)	6765	6765	6656	6673
Spectral Class[c]	F2-F3V	F2-F3V	F3-F4V	F3-F4V

a: E(B–V) = 0.0175 ±0.0005. b: T_{eff1} interpolated and spectral class assigned from Pecaut and Mamajek (2013). c: Mean value for $(B–V)_0$ = 0.393 ± 0.014; T_{eff1} = 6705 K; Spectral type = F2 to F3V.

Table 5 Fourier coefficients derived from Vmag light curve using UNIQUE[a].

Coefficient	*Calculated Value*	*Library Value*
a_0	+0.848932	+0.850691
a_1	–0.008729	–0.006636
a_2	–0.165170	–0.166897
a_3	–0.006588	–0.008652
a_4	–0.030641	–0.024858
a_5	–0.001247	–0.000322
a_6	–0.005090	–0.006625
a_7	–0.001790	–0.001988
a_8	+0.002385	+0.001871
a_9	–0.002313	–0.001730
a_{10}	+0.003141	+0.002698

a: Fit difference = 0.007449 corresponds to q = 0.225, f = 0.5, i = 79°.

from TYC 01963-0488-1 was primarily accomplished using the program PHOEBE 0.31a (Prša and Zwitter 2005). The model selected was for an overcontact binary not in thermal contact (Mode 3) and each curve was weighted based upon observational scatter. Bolometric albedo ($A_{1,2}$ = 0.5) and gravity darkening coefficients ($g_{1,2}$ = 0.32) for cooler stars (< 7500 K) with convective envelopes were assigned by theory according to Ruciński (1969) and Lucy (1967), respectively. The effective temperature of the more massive primary star was fixed (T_{eff1} = 6705 K) according to the earlier designation as spectral type F2V to F3V. Following any change in the effective temperature for the secondary (T_{eff2}), new logarithmic limb darkening coefficients (x_1, x_2, y_1, y_2) were interpolated according to Van Hamme (1993). All parameters except for T_{eff1}, $A_{1,2}$, and $g_{1,2}$ were allowed to vary during DC iterations. Roche modeling was initially seeded with q = 0.225 and i = 79° from UNIQUE (Hambálek and Pribulla 2013) and a lower effective temperature for the secondary (T_{eff2} = 6600 K) in order to comply with the definition of an A-type system. This assessment included synthesis of light curves for TYC 01963-0488-1 with and without the incorporation of a cool spot to address the so-called O'Connell effect (Max I brighter than Max II). The possibility of hot spots which can also produce LC asymmetry cannot be discounted; however, the appearance of cold spot(s) can be persistent and could explain the same Max II asymmetry observed between 1999 and 2000 by the ROTSE-I survey (Akerlof *et al.* 2000).

3.5. Modeling results

3.5.1. Light curve analysis

The initial estimates for q, i, and T_{eff2} quickly converged to best fit Roche model solutions. In this case the values (q and i) derived from UNIQUE were reasonably close to the final values determined from Roche modeling (Table 6). Corresponding unspotted (Figure 4) and spotted (Figure 5) simulations reveal that the addition of a cool spot on the less massive secondary star resulted in a modestly improved fit (χ^2) of these multi-color data. A pictorial model rendered with BM3 using the physical and geometric elements from the system with a cool spot on the secondary star is shown in Figure 6. After a best model fit was found, values and errors for T_{eff2}, i, q, and $\Omega_{1,2}$ were further examined using the PHOEBE scripter in which the WD minimization program (DC) was programmatically executed 1,000 times (Bonanos 2009). During each heuristic scan, input parameter values were updated for the next iteration and the formal error derived from the standard deviations; a representative example (Figure 7) illustrates the probabilistic relationship between q, i, and $\Delta\chi^2$. The fairly steep boundary which defines the 99.99% confidence interval ($\Delta\chi^2$ = 15.1) is consistent with a well-constrained value for q (0.248 ± 0.002).

The fill-out parameter (f), which is a measure of the shared photospheric volume between each star, was calculated according to Bradstreet (2005) as:

$$f = \frac{(\Omega_{inner} - \Omega_{1,2})}{(\Omega_{inner} - \Omega_{outer})} \quad (2)$$

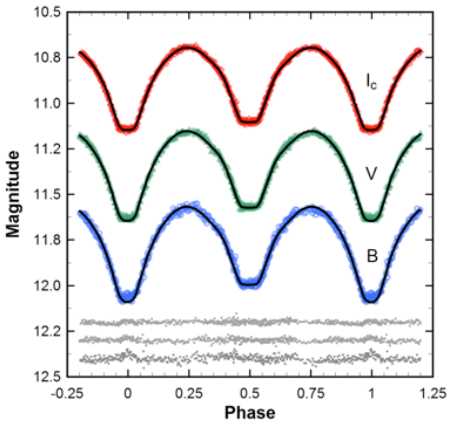

Figure 4. Synthetic fits (solid-line) of TYC 01963-0488-1 light curves (B-, V-, and I_c-mag.) produced from CCD data collected at UO during 2015. The Roche model assumed an A-subtype overcontact binary with no spots; residuals from the model fits are offset at the bottom of the plot to keep the values on scale.

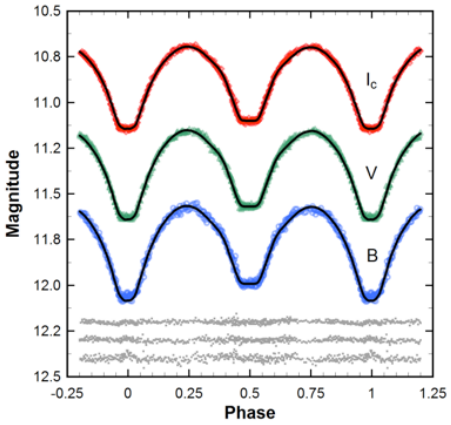

Figure 5. Synthetic fits (solid-line) of TYC 01963-0488-1 light curves (B-, V-, and I_c-mag.) produced from CCD data collected at UO during 2015. The Roche model assumed an A-subtype overcontact binary with a cool spot on the secondary; residuals from the model fits are offset at the bottom of the plot to keep the values on scale.

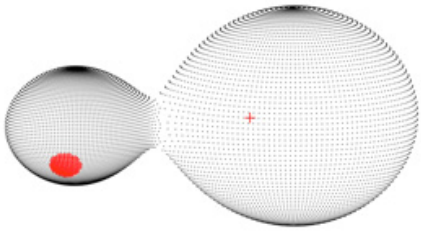

Figure 6. 3-D spatial model (φ = 0.79) of TYC 01963-0488-1 generated from 2015 photometric data showing the location of a cool spot on the secondary star.

where Ω_{outer} is the outer critical Roche equipotential, Ω_{inner} is the value for the inner critical Roche equipotential, and $\Omega = \Omega_{1,2}$ denotes the common envelope surface potential for the binary system. Since the fill-out value (~ 0.34) for TYC 01963-0488-1 lies between $0 < f < 1$, the system is defined as an overcontact binary. This is in contrast to semi-detached and detached systems where $f = 0$ and $f < 0$, respectively.

Table 6. Synthetic light curve parameters employed for Roche modeling and the geometric elements determined when assuming that TYC 01963-0488-1 is an A-type W UMa variable.

Parameter	*No Spot*	*Cool Spot (Secondary Star)*
T_{eff1} (K)[a]	6705	6705
T_{eff2} (K)[b]	6518 ± 18	6544 ± 13
q (m_2 / m_1)[b]	0.251 ± 0.003	0.248 ± 0.002
A[a]	0.5	0.5
g[a]	0.32	0.32
$\Omega_1 = \Omega_2$ [b]	2.302 ± 0.007	2.294 ± 0.004
i° [b]	81.61 ± 0.17	81.99 ± 0.57
$A_S = T_S / T$ [c]	—	0.86 ± 0.03[d]
Θ_S (spot co-latitude)[c]	—	122 ± 6[d]
φ_S (spot longitude)[c]	—	240 ± 5[d]
r_S (angular radius)[c]	—	14.0 ± 2[d]
$L_1 / (L_1 + L_2)_B$ [d,e]	0.8006 ± 0.0011	0.7980 ± 0.0005
$L_1 / (L_1 + L_2)_V$ [d,e]	0.7915 ± 0.0009	0.7903 ± 0.0004
$L_1 / (L_1 + L_2)_{Ic}$ [d,e]	0.7833 ± 0.0007	0.7833 ± 0.0004
r_1 (pole)[d]	0.4817 ± 0.0004	0.4829 ± 0.0005
r_1 (side)[d]	0.5242 ± 0.0006	0.5258 ± 0.0008
r_1 (back)[d]	0.5522 ± 0.0007	0.5538 ± 0.0010
r_2 (pole)[d]	0.2615 ± 0.0012	0.2609 ± 0.0011
r_2 (side)[d]	0.2740 ± 0.0015	0.2735 ± 0.0013
r_2 (back)[d]	0.3191 ± 0.0031	0.3190 ± 0.0029
Fill-out factor	33.67%	34.68%
χ^2 (B)[f]	0.003294	0.003094
χ^2 (V)[f]	0.002768	0.002782
χ^2 (I_c)[f]	0.005724	0.005574

a: Fixed during DC.
b: Error estimates for q, i, $\Omega_1 = \Omega_2$, and T_{eff2} from heuristic scanning .
c: Spot temperature, location, and size parameters in degrees.
d: Error estimates for spot parameters, $L_1 / (L_1 + L_2)$, r_1, and r_2 (pole, side and back) from WDWint v5.6a (Nelson 2009).
e: Bandpass dependent fractional luminosity; L_1 and L_2 refer to luminosities of the primary and secondary stars, respectively.
f: Monochromatic best Roche model fits ($\chi 2$) from PHOEBE 0.31a (Prša and Zwitter 2005).

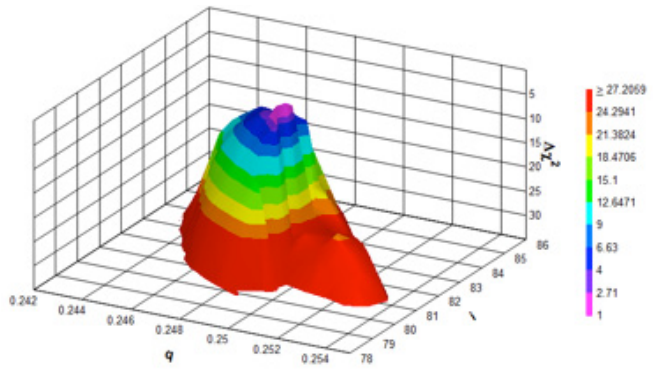

Figure 7. Probability contour illustrating the sharply defined surface boundaries for a best fit when mass ratio (q) and the orbital inclination (i) are iteratively adjusted during DC. Randomized q and i values (n=1000) were generated within ± 4% of the nominal input values for q (0.248) and i (81.99°). The parameter $\Delta\chi^2$ is a function of confidence level such that when $\Delta\chi^2$ =1 the probability in a paired comparison is 68.3% (1σ).

3.6. Absolute Parameter Estimates

Absolute parameters (Table 7) were derived for each star in this A-type W UMa binary system using results from the best fit simulation (spotted model) of the 2015 LC. In the absence of RV data ($v_{1r} + v_{2r}$), total mass can not be calculated directly. However, stellar mass and radii from binary systems have been tabulated over a wide range of spectral types (Harmanec 1988) where the primary star (T_{eff1} = 6705 K) in TYC 01963-0488-1 is estimated to have a mass of 1.48 ± 0.06 $M_\odot$. Alternatively, two different empirical period-mass relationships for W UMa-binaries have been reported by Gazeas and Stępień (2008) and Qian (2003). According to Gazeas and Stępień (2008) the mass of the primary star (M_1) can be determined from the expression (3):

Table 7. Absolute parameters for TYC 01963-0488-1 using results from the 2015 spotted Roche model.

Parameter	*Primary*	*Secondary*
Mass ($M_\odot$)	1.46 ± 0.07	0.36 ± 0.02
Radius ($R_\odot$)	1.46 ± 0.02	0.78 ± 0.01
a ($R_\odot$)	2.91 ± 0.04	—
Luminosity ($L_\odot$)	3.88 ± 0.09	1.00 ± 0.04
M_{bol}	3.28 ± 0.024	4.75 ± 0.024
Log (g)	4.27 ± 0.023	4.21 ± 0.024

$$\log M_1 = (0.755 \pm 0.059) \log P + (0.416 \pm 0.024), \quad (3)$$

while the mass of the secondary (M_2) can be similarly calculated from the orbital period (P) with the following relationship (4):

$$\log M_2 = (0.352 \pm 0.166) \log P - (0.262 \pm 0.067) \quad (4)$$

This leads to M_1 = 1.37 ± 0.1 $M_\odot$ for the primary and M_2 = 0.405 ± 0.086 $M_\odot$ for the secondary star. The value for the photometrically determined mass ratio (q_{ph} = 0.248 ± 0.002) from this study is contained within the mass ratio and error (q = 0.296 ± 0.066) calculated using equations 3 and 4. Another mass-period relationship (equation 5) was derived by Qian (2003) and largely corresponds to A-type W UMa systems where $M_1 > 1.35\ M_\odot$ and P > 0.41 d.

$$\log M_1 = 0.761\ (\pm 0.150) + 1.82\ (\pm 0.28) \times P \quad (5)$$

In this case the solution leads to a somewhat higher estimate for the primary star mass (M_1 = 1.54 ± 0.20). The average of all three values (M_1 = 1.46 ± 0.07) was used for subsequent determinations of M_2, semi-major axis (a), volume-radius (r_L), bolometric magnitude (M_{bol}), and distance (pc) to TYC 0163-0488-1. The semi-major axis, $a(R_\odot)$ = 2.91 ± 0.04, was calculated according to Kepler's third law where:

$$a_3 = \frac{(G \times P^2\ (M_1 + M_2))}{(4\pi^2)} \quad (6)$$

According to the expression (7) derived by Eggleton (1983), the effective radius of each Roche lobe (r_L) can be calculated to within an error of 1% over the entire range of mass ratios ($0 < q < \infty$):

$$r_L = \frac{0.49q^{2/3}}{0.6q^{2/3} + \ln(1 + q^{1/3})} \quad (7)$$

Volume-radius values were determined for the primary ($r_1 = 0.5021 \pm 0.0001$) and secondary ($r_2 = 0.2670 \pm 0.0001$) stars. The absolute radii for both binary constituents can then be calculated where $R_1 = a \times r_1 = 1.46 \pm 0.02\ R_\odot$ and $R_2 = a \times r_2 = 0.78 \pm 0.01\ R_\odot$. The bolometric magnitude (M_{bol}) and luminosity ($L_{1,2}$) in solar units ($L_\odot$) for the primary and secondary stars were calculated from well-established relationships where

$$M_{bol1,2} = 4.75 - 5 \log \left(\frac{R_{1,2}}{R_\odot} \right) - 10 \log \left(\frac{T_{1,2}}{T_\odot} \right) \quad (8)$$

and

$$L_{1,2} = \left(\frac{R_{1,2}}{R_\odot} \right)^2 \left(\frac{T_{1,2}}{T_\odot} \right)^4 \quad (9)$$

Assuming that $T_{eff1} = 6705$ K, $T_{eff2} = 6544$ K and $T_\odot = 5778$ K, the bolometric magnitudes are $M_{bol1} = 3.278 \pm 0.024$ and $M_{bol2} = 4.754 \pm 0.024$, while the solar luminosities for the primary and secondary are $L_1 = 3.88 \pm 0.09\ L_\odot$ and $L_2 = 1.00 \pm 0.04\ L_\odot$, respectively.

The distance to TYC 0163-0488-1 (438 ± 5 pc) was estimated using the distance modulus Equation (10) corrected for interstellar extinction. In this case V mag at Min II ($m = 11.57 \pm 0.01$) is defined when the primary totally eclipses the secondary, and M_V is the absolute magnitude derived using the bolometrically corrected magnitude ($M_{bol1} - BC$). The interstellar extinction ($A_V = 0.05425 \pm 0.00155$) was determined from E(B–V), the color excess previously described in section 3.3 where E = 3.1.

$$d(pc) = 10^{(((m - M_V) - A_V + 5) / 5)} \quad (10)$$

Another value for distance (399 ± 36 pc) was calculated according to the empirical expression (11)

$$\log D = 0.2 \times V_{max} - 0.18 \times \log P - 1.6\,(J–H) + 0.56 \quad (11)$$

derived by Gettel *et al.* (2006) from a ROTSE-I catalog of overcontact binary stars where D is distance in parsecs, P is the orbital period in days, $V_{max} = 11.17 \pm 0.01$, and (J–H) is the 2MASS color for TYC 01963-0488-1. The combined mean distance to this system is therefore estimated to be 419 ± 18 pc.

4. Conclusions

CCD-based photometric data captured in B, V, and I_c passbands produced five new times-of-minimum for the W UMa binary system TYC 01963 0488-1. A first epoch (HJD_0) linear ephemeris for TYC 01963-0488-1 was established for this system; many more years of data will likely be required to determine whether there are any secular changes in orbital period. The weight of evidence from this study and other surveys suggested that the effective temperature of the most luminous star is 6705 K and corresponds to F2V-F3V spectral class. The greatest challenge to definitive Roche modeling of the rapidly expanding catalog of newly discovered W UMa binaries is the absence of published RV data to unequivocally determine a mass ratio (q) and subtype (A or W). Fortuitously this system experiences clearly defined total eclipses which help constrain a photometrically determined mass ratio result ($q \sim 0.25$). Since maximum light at $\varphi = 0.25$ and 0.75 was not equal, a cool-spot solution was necessary to achieve the best Roche model fits for TYC 01963-0488-1. Similar LC behavior observed between 1999 and 2000 suggests that this system has an active photosphere. Until which time RV data become publically available, these Roche model fits and any absolute parameters derived for this W UMa binary are subject to some uncertainty. The sum total of all data collected thus far suggests that TYC 01963-0488-1 is most likely an A-type W UMa variable located over 400 pc from our home planet. Public access to any data associated with this research can be obtained by request (mail@underoakobservatory.com).

5. Acknowledgements

This research has made use of the SIMBAD database, operated at Centre de Données astronomiques de Strasbourg, France, the Northern Sky Variability Survey hosted by the Los Alamos National Laboratory, and the International Variable Star Index maintained by the AAVSO. The diligence and dedication shown by all associated with these organizations is very much appreciated. The author gratefully acknowledges the comments and helpful suggestions that the referee offered to improve the overall quality of this research paper.

References

Akerlof, C., *et al.* 2000, *Astron. J.*, **119**, 1901.

Berry, R., and Burnell, J. 2011, "Astronomical Image Processing for Windows," version 2.4.0, provided with *The Handbook of Astronomical Image Processing*, Willmann-Bell, Richmond, VA.

Binnendijk, L. 1970, *Vistas Astron.*, **12**, 217.

Bonanos, A. 2009, *Astron. J.*, **691**, 407.

Bradstreet, D. H. 2005, in *Society for Astronomical Sciences, 24th Annual Symposium*, Society for Astronomical Sciences, Rancho Cucamonga, CA, 23.

Bradstreet, D. H., and Steelman, D. P. 2004, BINARY MAKER 3, Contact Software (http://www.binarymaker.com).

Eggleton, P. P. 1983, *Astrophys. J.*, **268**, 368.

Gazeas, K., and Stępień, K. 2008, *Mon. Roy. Astron. Soc.*, **390**, 1577.

Gettel, S. J., Geske, M. T., and McKay, T. A. 2006, *Astron. J.*, **131**, 621.

Hambálek, L., and Pribulla, T. 2013, *Contrib. Astron. Obs. Skalnatè Pleso*, **43**, 27.

Harmanec, P. 1988, *Bull. Astron. Inst. Czechoslovakia*, **39**, 329.

Hoffman, D. J., Harrison, T. E., and McNamara, B. J. 2009, *Astron. J.*, **138**, 466.

Kwee, K. K., and van Woerden, H. 1956, *Bull. Astron. Inst. Netherlands*, **12**, 327.

Lucy, L. B. 1967, *Z. Astrophys.*, **65**, 89.

Minor Planet Observer. 2015, MPO Software Suite (http://www.minorplanetobserver.com), BDW Publishing, Colorado Springs.

Nelson, R. H. 2009, WDWINT5.6A, astronomy software by Bob Nelson (http://members.shaw.ca/bob.nelson/software1.htm).
Pecaut, M. J., and Mamajek, E. E. 2013, *Astrophys. J., Suppl. Ser.*, **208**, 1.
Pribulla, T. 2012, in *From Interacting Binaries to Exoplanets: Essential Modelling Tools*, IAU Symp. 282, eds. M. T. Richards, I. Hubeny, Cambridge Univ. Press, Cambridge, 279.
Prša, A., and Zwitter, T. 2005, *Astrophys. J.*, **628**, 426.
Qian, S. 2003, *Mon. Not. Roy. Astron. Soc.*, **342**, 1260.
Ruciński, S. M. 1969, *Acta Astron.*, **19**, 245.
Schlafly, E. F., and Finkbeiner, D. P. 2011, *Astrophys. J.*, **737**, 103.
Schlegel, D. J., Finkbeiner, D. P., and Davis, M. 1998, *Astrophys. J.*, **500**, 525.
Schwarzenberg-Czerny, A. 1996, *Astrophys. J., Lett. Ed.*, **460**, L107.
Skelton, P. L., and Smits, D. P. 2009, *South African J. Sci.*, **105**, 120.
Software Bisque. 2011, CCDSOFT CCD control software (http://www.bisque.com).
Terrell, D., and Wilson, R. E. 2005, *Astrophys. Space Sci.*, **296**, 221.
Van Hamme, W. 1993, *Astrophys. J.*, **106**, 2096.
Vanmunster, T. 2006, Light Curve and Period Analysis Software, PERANSO v.2.5 (http://www.peranso.com/), CBA Belgium Observatory.
Warner, B. D. 2007, *Minor Planet Bull.*, **34**, 113.
Watson, C., Henden, A. A., and Price, C. A. 2014, AAVSO International Variable Star Index VSX (Watson+, 2006–2014; http://www.aavso.org/vsx).
Wilson, R. E. 1979, *Astrophys. J.*, **234**, 1054.
Wilson, R. E. and Devinney, E. J. 1971, *Astrophys. J.*, **166**, 605.
Wozniak, P. R., *et al.* 2004, *Astron. J.*, **127**, 2436.
Yakut, K., and Eggleton, P. P. 2005, *Astrophys. J.*, **629**, 1055.